

## A New Approach in the Decellularization of Porcine Skin for Tissue Engineering Applications

Jean Andrea Nicola T. Banzon<sup>1</sup>, Nathan Matthew S. Co<sup>1</sup>, Glynis Jen J. Dawa<sup>1</sup>, Anna Paula S. Policarpio<sup>1</sup>, Aika Angel F. Ubando<sup>1</sup>, and Mariquit M. De Los Reyes\*

<sup>1</sup> *Department of Biology, De La Salle University, Taft Avenue, Manila*

*\*Corresponding Author: mariquit.delosreyes@dlsu.edu.ph*

**Abstract:** Bioengineering is key to addressing issues in regenerative medicine, with 3D bioprinting using extracellular matrix (ECM) derived from decellularized skin at the forefront of different tissue engineering applications. The main objective of this study was to develop a protocol that would efficiently delipidize and decellularize porcine dermis by combining the use of 70% isopropanol and 0.1% sodium dodecyl sulfate (SDS) with sonication. The protocol also aimed to preserve the structural integrity of the ECM similar to its native state. The loss of cells, preservation of ECM fibers, and ECM architecture were the criteria initially used to evaluate the effectiveness of the protocol. Hematoxylin & Eosin (H&E) staining and a modified histological scoring were done for this purpose. Based on this scoring system, 240 W and 9 hr sonication time were found to be the most ideal decellularization conditions. The native samples, as well as those obtained using the protocol conditions that obtained the highest average score from the criteria above (240 W and 9 hr), were analyzed using scanning electron microscopy with energy-dispersive x-ray (SEM-EDX) and attenuated total reflectance - Fourier transform infrared (ATR-FTIR) spectroscopy. The SEM images showed possible degradation of the decellularized porcine skin. On the other hand, the results of ATR-FTIR spectroscopy showed that after decellularization, functional groups found in the native samples were retained, implying that the decellularized porcine skin's structural integrity was preserved. To date, based on available sources, this may be the first report on a protocol utilizing a combination of alcohol and detergent, coupled with sonication, for decellularizing porcine dermis.

**Key Words:** decellularization; porcine dermis; sonication; ECM

## 1. INTRODUCTION

Constructing biological mimics to replace damaged tissues and organs in order to regain or improve biological functions is the primary goal of tissue engineering. Among the leading techniques used in tissue engineering is 3D bioprinting, specifically, the use of bioinks in regenerative medicine. Bioinks that are 3D-bioprinted can find use in tissue reconstruction, drug screening, disease modeling, and in vitro transplantation. For example, this is most relevant in the fabrication of personalized wound dressings. However, due to the possible physiological complexity of tissues and organs under investigation, the production of bioink may entail a high cost. In order to address this, there is a growing trend in studying bioink materials from natural products, such as animal skin, that may be rich in biological molecules that can enhance the healing of affected tissues.

The skin, specifically the dermis, is mainly composed of connective tissues, collagen, and elastic fibers and these materials can be widely used in tissue engineering (Xu et al., 2020). The dermal skin of pigs can also be a good source of collagen as it resembles the anatomy of humans (Summerfield et al., 2015). Decellularization is a required step to utilize the porcine skin as a potential bioink component. Here, the removal of the cellular components of scaffolds while maintaining both the macrostructure and microstructure of the extracellular matrix is performed using physical, chemical, and enzymatic means (Taylor et al., 2020).

The main objective of this study was to develop a protocol that could effectively decellularize porcine skin, combining the use of 0.1% SDS, 70% isopropanol solution, and sonication. Alcohols may be useful in delipidizing the tissue samples. Improvements on decellularization techniques are crucial as the resulting material can be potentially used as a bioink component for 3D bioprinting purposes in additive manufacturing techniques in tissue engineering. Most of the published methodologies use SDS in combination with other techniques, but not the use of alcohol and sonication. Hence, this paper may be the first report on the use of SDS-alcohol-sonication in decellularization.

## 2. METHODOLOGY

### 2.1 Preparation of Porcine Skin

The porcine skin was purchased from a reputable meat dealer (Marky's Meat Shop, BF Resort Village, Las Piñas City). The dermis was isolated from the entire porcine skin and sliced into uniform sizes, approximately 5 mm x 5 mm, using a surgical blade. To remove any debris, the cut-up dermis was submerged in 100 mL distilled water and agitated using a magnetic stirrer at 100 rpm, room temperature (21°C), and 5 min.

### 2.2 Decellularization

The decellularization solution was prepared by combining 0.1% SDS ( $\geq 98.5\%$ , Sigma-Aldrich) with 70% isopropanol (RCI Labscan AR1162-G2.5L Propan-2-ol). The decellularization protocol consisted of two set-ups: (1) control set-up where samples were submerged in 70% isopropanol-0.1% SDS solution for 9 hr, and (2) treatment set-up where samples were submerged in 70% isopropanol-0.1% SDS solution for 9 hr with different sonicator (CP2600, Crest Ultrasonics) power per run (180 W, 240 W). For every three-hour interval, defined cut samples were removed from the solution, and the volume of the isopropanol-SDS solution was adjusted accordingly (5 mL of solution for every 1 piece porcine sample). This eliminated the factor that the high volume of solution for the second and third intervals introduced changes in the decellularization environment. The final step consisted of two stages of washing with agitation: (1) 50 mL of 1% Triton-X (extra pure, LOBA Chemie PVT, Ltd.) at 100 rpm, 21°C, and 1 hr, to remove the SDS residue, and (2) 50 mL of distilled water at 100 rpm, 21°C, 30 min, to remove the Triton-X residues (Mondragon et al., 2021). The porcine skin that was not exposed to the isopropanol-SDS solution served as native samples.

### 2.3 Storage of Decellularized Porcine Skin

Samples (native and decellularized) were stored in 20 mL of formalin for H&E staining, and 20 mL of phosphate buffered saline (pH 7.4, Sigma-Aldrich) for SEM-EDX (Thermo Scientific™ Phenom XL Desktop SEM) and ATR-FTIR (Perkin Elmer FT-IR Spectrometer and Spectrum 10 Software) analyses. The H&E scoring was first conducted to assess the protocol's effectiveness based on three defined criteria:

(1) loss of cells, (2) preservation of tissue fibers, and (3) tissue architecture. Lyophilized samples were also examined under SEM-EDX for structural and elemental analysis, and under ATR-FTIR spectroscopy for the identification of functional groups that were present in the samples.

### 3. RESULTS AND DISCUSSION

#### 3.1 Macroscopic Assessment

Prior to decellularization, images of the native samples were taken for baseline data to assess for any morphological changes in the decellularized samples. Porcine skin lacks the presence of melanocytes which mainly explains its pale white color appearance (Tsatmali et al., 2002). Hence, it may be challenging to evaluate the efficiency of decellularization based on color changes alone. For example, in the paper of Manalastas et al. (2020) using a kidney, the color change was reliable since the whole kidney changed from reddish brown to translucent white after a successful decellularization. However, in the study, it was observed that longer sonication time (i.e., 6 and 9 hr) resulted to a relatively firmer and lighter tissue sample as compared to the native samples. This could be attributed to the efficient removal of lipid residues during the process of decellularization, although visual observations alone may not be conclusive.

#### 3.2 Histological Analysis

Three criteria were defined in the study and were used as the basis for assessing the effectiveness of the experimental protocol: (1) loss of cells, (2) preservation of tissue fibers, and (3) overall condition of the tissue architecture. Criteria 2 and 3 could imply the presence of collagen, which is the most abundant ECM protein in dermal tissues (Xu et al., 2020). Ten random images to represent each experimental condition were used in the assessment and were scored from 0 to 3 by nine scorers. For all criteria, 0 was the lowest score, implying decellularization did not occur (or occurred but to a minimum degree), and 3 was the highest, indicating that decellularization has effectively occurred. The total scores per image (per condition/parameter) were added together and the highest and lowest averages were noted. Table 1 shows the experimental condition that scored the highest based on the imaging criteria used.

Table 1. Average scores per criterion for the condition that scored the highest (240 W, 9 hr)

Criteria	Scores of Ten Images (%)
1. Cell Removal	76.25%
2. Preservation of ECM Fibers	80.00%
3. ECM Architecture	86.25%
<b>Average score based on all three criteria (240 W, 9 hr)*</b>	<b>81.00%</b>

\*Samples that scored the highest in all three criteria were those sonicated at 240 W for 9 hr

Based on the results provided above, the decellularization condition that scored the highest in the cell removal criterion was 240 W and 9 hr. It was also observed in the study that with respect to criterion 2 (preservation of the protein, presumably, collagen ECM fibers in the matrix), non-sonicated porcine skin showed a higher score compared to those that were sonicated. This pertains to the sample that was only exposed to 0.1% SDS and 70% isopropanol for 9 hr without any sonication (0 W). Given that decellularization using sonication was done, both removal of cells and disruption of ECM occurred. It has been proven that all decellularization procedures may disrupt the ECM structure and orientation because cellular components are also extracted in the process (Crapo et al., 2011).

Figure 1 compares the cell content of native sample versus decellularized porcine skin (240 W, 9 hr).

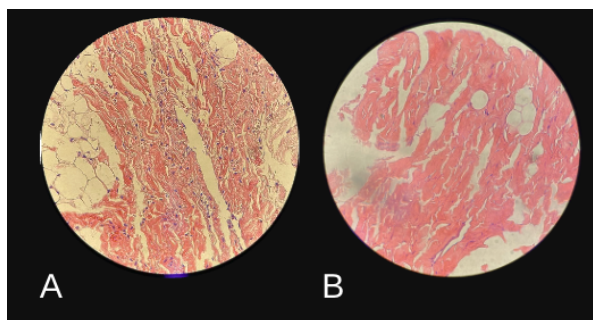


Fig. 1. Representative H&E-stained images (400X) of the porcine dermis (A: native samples, B: decellularized at 240 W for 9 hr).

Sonicator power coupled with 0.1% SDS and 70% isopropanol solution may be an effective approach to facilitate the removal of cells in the tissues. However, prolonged exposure to SDS can contribute to damage in the ECM architecture (Bertanha et al., 2014). Reducing the exposure of the bioscaffold or tissue to SDS, with the aid of appropriate sonication power, increases the chances of preserving the ECM (Manalastas et al., 2020).

In general, sonication decreases the exposure time to detergents and other chemicals through the cavitation of microbubbles that produce shockwaves, which can disrupt the cell membrane and facilitate the removal of cells (Saranya et al., 2014). Therefore, higher sonicator power increases the microbubbles, which, in turn, allows for more efficient cell removal. However, increasing the sonicator power and exposure time may also lead to prolonged exposure to microbubble cavitation and its accompanying high temperatures, resulting in the disruption of the structural integrity and denaturation of proteins in the sample (Manalastas et al., 2020).

### 3.3 SEM-EDX Analysis

As determined from the histological scoring, samples obtained using the decellularization condition that scored the highest (240 W, 9 hr) were analyzed under SEM-EDX to examine the microstructures and to determine its elemental composition. The photos were captured at 300x magnification, since, according to the technician, the samples started to degrade at magnifications above 1000x. The results were compared to the native samples and are presented in Figure 2.

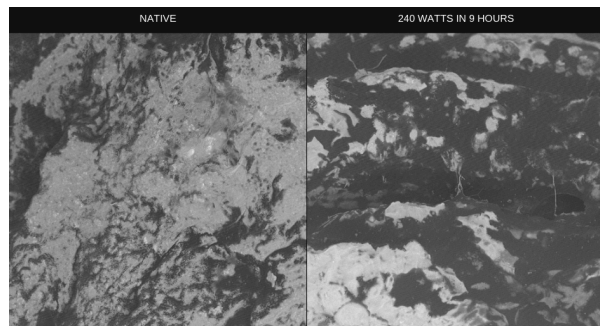


Fig. 2. SEM micrographs of porcine skin (left: native sample; right: exposed to 240 W, 9 hr of sonication); 300x magnification.

In a study by Ventura et al. (2019), ECM characterized under SEM revealed a dense structure for the native ECM, but a less dense structure with minimal fibrous network in the case of decellularized ECM. In this study, the same was observed with only a minimal number of detached fibers seen in the decellularized porcine skin. Hence, this suggests that the 240 W and 9 hr condition did not preserve most of the fibers in the native samples. This may be due to the combined effects of prolonged use of both sonication and chemical agents (SDS and alcohol).

For the elemental composition of the native and decellularized samples (240 W, 9 hr), there were only minimal amounts of trace elements detected. Samples had traces of carbon (C) and oxygen (O). Comparing this to the native samples, it was evident that some elements such as sodium (Na) and chlorine (Cl) were lost after decellularization. Previous studies showed that the loss of these ions resulted when they aggregated with SDS (Sammalkorpi et al., 2009). The absence of a detectable level of nitrogen implies that protein content decreased both in the native and the decellularized porcine skin. It was possible that the region of interest evaluated lacked detectable nitrogen that could be measured. The absence of nitrogen may also suggest that the protein might have been degraded either during the decellularization procedure or during storage prior to the analysis. The presence of any collagen and ECM proteins was further analyzed and confirmed through ATR-FTIR spectroscopy.

### 3.4 ATR-FTIR Analysis

The ATR-FTIR analysis was done to compare the functional groups present in the tissue samples before and after decellularization. Subjected to ATR-FTIR analysis were the native samples and the decellularized samples under 240 W, 9 hr, the decellularization conditions that scored the highest in the histological analysis which was the preliminary investigation used to characterize and screen the samples. Generally speaking, the spectra of the native and treated samples (sonicated at 240 W for 9 hr) exhibited consistent trends compared to a related study conducted by Ventura et al. (2019).

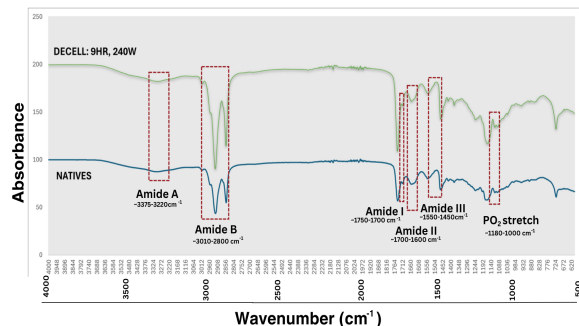


Fig. 3. ATR-FTIR spectra of treated and untreated porcine skin (blue: native; green: 240 W, 9 hr; red dashed lines show peaks indicating functional groups)

Table 2 also shows the results of the ATR-FTIR analysis of porcine skin with the corresponding functional groups identified in specific wavenumbers where peaks were found.

Table 2. Wavenumbers (left column) of functional groups (right column) present in porcine skin based on ATR-FTIR analysis.

Band	Functional Groups
~3375-3220 cm <sup>-1</sup>	<b>Amide A</b> of phospholipids, glycolipids, & fatty acids (Ventura et al., 2019)
~3010-2800 cm <sup>-1</sup>	<b>Amide B</b> of phospholipids, glycolipids, & fatty acids (Ventura et al., 2019)
~1750-1700 cm <sup>-1</sup>	C=O of <b>Amide I</b> (Stani et al., 2020)
~1700-1600 cm <sup>-1</sup>	N-H & C-N of <b>Amide II</b> (Koochakzaei et al., 2018)
~1550-1450 cm <sup>-1</sup>	N-H, C-N, & C-C of <b>Amide III</b> (Smith, 2023)
~1180-1000 cm <sup>-1</sup>	Phosphate nucleic acids of <b>PO<sub>2</sub> Stretch</b> (De La Arada et al., 2020)

The structural components of the decellularized samples were maintained as indicated by identical infrared radiation (IR) patterns seen compared to the native samples. While the micrographs from the SEM analysis were inconclusive with respect to the preservation of protein fibers, the

functional groups found in the native samples remained present in the decellularized samples based on the FTIR results. Retention of structural integrity was also evident on the spectral graph.

The peaks where amides A and B are present are indicative of phospholipids, glycolipids, and fatty acids (Ventura et al., 2019). The fingerprint region is found in peaks 1500-600 cm<sup>-1</sup> (Heydari et al., 2023; Tiquia-Arashiro et al., 2023), or usually in overlapping bands. This shows the spectral signature of the given sample as it contains the fundamental vibrations of all compounds (Magalhães et al., 2021).

Amide A and B are necessary constituents of ECM that should be preserved since they are found in Type I collagen which is essential in formulating bioink materials (Stepanovska et al., 2021). The observed amide A band is related to the N-H stretching vibration indicative of the presence of intermolecular hydrogen bonding (Noorzai et al., 2019). Meanwhile, the amide B band is due to the CH<sub>2</sub> stretching vibration which can be found abundantly in SDS (Sperline, 1997; Sperline, Song, & Freiser, 1997).

As shown in previous studies, various amide bands including amides I, II, and III are exhibited in the IR spectrum by Type I collagen, which is the protein abundantly found in porcine skin (Liu et al., 2010; Stani et al. 2019). The Amide I band indicates the C=O stretching vibration which can provide important information on the secondary structure of proteins and peptides (Stani et al., 2020). Amide II indicates the N-H bending and C-N stretching while Amide III indicates all that the Amide II band does, but it additionally indicates C-C stretching. Both of which can provide significant information regarding the overall structure of the entire spectrum.

Additionally, a symmetric PO<sub>2</sub> stretch of phosphate salt nucleic acid DNA and RNA is also evident. The phosphate group stretch can provide valuable information about the molecular structure of the phosphate groups and their interactions among neighboring molecules (De La Arada et al., 2020). This may also be correlated to the presence of residual lipids in the decellularized samples, expounding on how the presence of water influences how phosphate groups and lipid residues interact.

As observed in the graph, there is a slight increase in the absorbance level of the decellularized sample which may indicate the presence of lipids due to incomplete decellularization or may just indicate an increase in water content. Hence, the presence of lipid residues in the decellularized samples may suggest that the samples were not completely delipidized, which may affect the biocompatibility and suitability of the sample as a potential bioink (Zhang et al., 2023). The delipidization not being complete could be due to the protocol used, that combined the delipidization and decellularization step, to limit the exposure of the samples to other chemicals besides the primary solution used (i.e. isopropanol-SDS).

Overall, the ATR-FTIR analysis showed that functional groups present in native samples were retained after the decellularization protocol. It was also likely that the structural integrity of the ECM was maintained post-decellularization. The presence of the amide bands I, II, and III confirmed the presence of collagen as these amide bands represent the fingerprint region of the whole FTIR spectra. In both native and decellularized samples, the peaks indicate phospholipids, proteins, glycolipids, peptides, and fatty acids. The traces of these lipid residues may still be present as evidenced by the PO<sub>2</sub> stretching. This showed that the new decellularization protocol used can successfully create a bioink component for future tissue engineering applications.

#### 4. CONCLUSIONS

In summary, a decellularization protocol involving the use of a chemical treatment (SDS-isopropanol solution) with sonication was used to decellularize porcine skin so that the treated components may be evaluated in terms of the presence and preservation of extracellular matrix (ECM), an important bioink biomaterial in tissue engineering applications. The most ideal decellularizing condition (240 W and 9 hr) was determined through histological analysis. Samples treated under these conditions were further characterized using SEM-EDX and ATR-FTIR spectroscopy in order to assess the structure, integrity, and components of any ECM molecules remaining after decellularization.

The SEM micrographs showed minimal protein fibers in the decellularized porcine skin. The EDX elemental composition analysis suggested possible protein degradation during the decellularization as shown by the absence of nitrogen, an important element present in proteins. However, the SEM-EDX results may be inconclusive since the region of interest selected during viewing is crucial in the analysis.

On the other hand, the ATR-FTIR spectra revealed the presence of various functional groups that were also present in native samples. Specifically, the results showed that the amide A, B, I, II, and III bands were observed in the decellularized samples, and this may be indicative of the presence of collagen in the treated tissues. However, the presence of a PO<sub>2</sub> stretch band is indicative of the presence of residual lipids, which suggests that samples were not completely delipidized.

Overall, further studies are needed to improve the protocol to achieve the ideal cell removal conditions while preserving the structural and architectural integrity of the porcine skin tissues. Complete delipidization of samples should also be targeted in future studies alongside decellularization to produce a potential bioink with biocompatible mechanical properties. Future studies may also use the results presented in this study as baseline data to produce decellularized porcine skin and dermis-derived bioink that can be useful in different tissue engineering applications. To date, based on available sources, this may be the first report on a new protocol involving the use of SDS-isopropanol with sonication for the decellularization of dermal porcine skin.

#### 5. ACKNOWLEDGMENTS

The assistance of the members of the DLSU Biomaterials and Tissue Engineering Laboratory (BiMaTEL) is greatly acknowledged, especially Mr. John Martin Mondragon, who also provided valuable insights during the conduct of the work. Likewise, the help of faculty and research assistants who scored the histological slides are recognized. For the H&E staining, the assistance of UP Manila Department of Pathology is acknowledged. For the ATR-FTIR analysis, the support of the Department of Science and Technology - Philippine Nuclear Research Institute (DOST-PNRI) is also acknowledged. Mr. Kyle Bitangcor and Mr. Paul Adrian Go both helped in interpreting the ATR-FTIR results.

## 6. REFERENCES

- AAT Bioquest (2021). Is SDS considered a detergent? <https://www.aatbio.com/resources/faq-frequently-asked-questions/Is-SDS-considered-a-detergent>
- Alberts, B., Johnson, A., Lewis, J., Raff, M., Roberts, K., & Walter, P. (2002). *The shape and structure of proteins*. Molecular Biology of the Cell - NCBI Bookshelf. <https://www.ncbi.nlm.nih.gov/books/NBK26830/>
- Bertanha, M., Moroz, A., Jaldin, R. G., Silva, R. A., Rinaldi, J. C., Golim, M. A., Felisbino, S. L., Domingues, M. A., Sobreira, M. L., Reis, P. P., & Deffune, E. (2014). Morphofunctional characterization of decellularized vena cava as tissue engineering scaffolds. *Experimental Cell Research*, 326(1), 103-111.
- Crapo, P. M., Gilbert, T. W., & Badylak, S. F. (2011). An overview of tissue and whole organ decellularization processes. *Biomaterials*, 32(12), 3233–3243. <https://doi.org/10.1016/j.biomaterials.2011.01.057>
- De La Arada, I., González-Ramírez, E. J., Alonso, A., Goñi, F. M., & Arrondo, J. R. (2020). Exploring polar headgroup interactions between sphingomyelin and ceramide with infrared spectroscopy. *Scientific Reports*, 10(1). <https://doi.org/10.1038/s41598-020-74781-8>
- Heydari, M., Colagar, A. H., & Sabour, D. (2023). Optimization of Affinity Chromatography Based on Sepharose 4B- chitin for Rapid Purification of *Urtica dioica* Agglutinin. PubMed, 21(3), e3364. <https://doi.org/10.30498/ijb.2023.339309.3364>
- Jha, S., Sharma, P.K., & Malviya, R. (2016). Liposomal drug delivery system for cancer therapy: advancement and patents. *Recent Pat. Drug Deliv. Formulation*, 10, 177–183.
- Liu, Y., Chen, J. Y., Shang, H. T., Liu, C. E., Wang, Y., Niu, R., Wu, J., & Wei, H. (2010). Light microscopic, electron microscopic, and immunohistochemical comparison of Bama minipig (*Sus scrofa domestica*) and human skin. *Comparative medicine*, 60(2), 142–148.
- Liu, Y., Huang, C., Wang, Y., Xu, J., Wang, G., & Bai, X. (2021). Biological evaluations of decellularized extracellular matrix collagen microparticles prepared based on plant enzymes and aqueous two-phase method. *Regenerative Biomaterials*, 8(2). <https://doi.org/10.1093/rb/rbab002>
- Magalhães, S., Goodfellow, B. J., & Nunes, A. (2021). FTIR spectroscopy in biomedical research: how to get the most out of its potential. *Applied Spectroscopy Reviews*, 56(8–10), 869–907. <https://doi.org/10.1080/05704928.2021.1946822>
- Manalastas, T. M., Dugos, N. P., Ramos, G. B., & Mondragon, J. M. (2020). Effect of decellularization parameters on the efficient production of kidney bioscaffolds. *Applied Biochemistry and Biotechnology*, 193(5), 1239–1251. <https://doi.org/10.1007/s12010-020-03338-2>
- Mondragon, J. S. (2022). Development and comparative characterization of hydrogel derived from the renal cortex and renal medulla of the decellularized kidney. Retrieved from [https://animorepository.dlsu.edu.ph/etdm\\_bio/18](https://animorepository.dlsu.edu.ph/etdm_bio/18)
- Noorzai, S., Verbeek, C. J. R., Lay, M. C., & Swan, J. (2019). Collagen Extraction from Various Waste Bovine Hide Sources. *Waste and Biomass Valorization*, 11(11), 5687–5698. <https://doi.org/10.1007/s12649-019-00843-2>
- Sammalkorpi, M., Karttunen, M., & Haataja, M. (2009). Ionic surfactant aggregates in saline solutions: sodium dodecyl sulfate (SDS) in the presence of excess sodium chloride (NaCl) or calcium chloride (CaCl<sub>2</sub>). *The Journal of Physical Chemistry. B*, 113(17), 5863–5870. <https://doi.org/10.1021/jp901228v>

- Saranya, N., Devi, P., Nithiyantham, S., & Jeyalaxmi, R. (2014). Cells disruption by ultrasonication. *BioNanoScience*, 4(4), 335–337.
- Shi, Q., Chen, C., Li, M., Chen, Y., Xu, Y., Hu, J., Liu, J., & Lu, H. (2021). Characterization of the distributions of collagen and PGs content in the decellularized book-shaped entheses scaffolds by SR-FTIR. *BMC Musculoskeletal Disorders*, 22(1). <https://doi.org/10.1186/s12891-021-04106->
- Sperline, R.P. (1997). Infrared spectroscopy study of the crystalline phases of sodium dodecyl sulfate. *Langmuir*, 13(14), 3715–3726.
- Sperline, R.P., Song, Y., & Freiser, H. (1997). Temperature dependent structure of adsorbed sodium dodecyl sulfate at the Al<sub>2</sub>O<sub>3</sub>/water interface. *Langmuir*, 13(14), 3727–3732.
- Stani, C., Vaccari, L., Mitri, E., & Birarda, G. (2020). FTIR investigation of the secondary structure of type I collagen: New insight into the amide III band. *Spectrochimica Acta. Part a, Molecular and Biomolecular Spectroscopy*, 229, 118006. <https://doi.org/10.1016/j.saa.2019.118006>
- Stepanovska, J., Supova, M., Hanzalek, K., Broz, A., & Matejka, R. (2021). Collagen Bioinks for bioprinting: A systematic review of hydrogel properties, bioprinting parameters, protocols, and bioprinted structure characteristics. *Biomedicines*, 9(9), 1137. <https://doi.org/10.3390/biomedicines9091137>
- Summerfield, A., Meurens, F., & Ricklin, M. E. (2015). The immunology of the porcine skin and its value as a model for human skin. *Molecular Immunology*, 66(1), 14–21. <https://doi.org/10.1016/j.molimm.2014.10.023>
- Sun, T., Zhang, Y.S., Pang, B., Hyun, D.C., Yang, M., & Xia, Y. (2014). Engineered nanoparticles for drug delivery in cancer therapy. *Angew. Chem*, 53, 12320–12364.
- Taylor, D., Lee, P., Barac, Y., Hochman-Mendez, C., & Sampaio, L. (2020). Chapter 15 - Decellularization of whole hearts for cardiac regeneration. *Emerging Technologies for Heart Diseases*, 1, 291-310. <https://doi.org/10.1016/B978-0-12-813706-2.00015-4>
- Tiquia-Arashiro, S., Li, X., Pokhrel, K., Kassem, A., Abbas, L., Coutinho, O., Kasperek, D., Najaf, H., & Opara, S. (2023). Applications of Fourier Transform-Infrared spectroscopy in microbial cell biology and environmental microbiology: advances, challenges, and future perspectives. *Frontiers in Microbiology*, 14. <https://doi.org/10.3389/fmicb.2023.130408>
- Tsatmali, M., Ancans, J., & Thody, A. J. (2002). Melanocyte function and its control by melanocortin peptides. *Journal of Histochemistry and Cytochemistry*, 50(2), 125–133. <https://doi.org/10.1177/002215540205000201>
- Ventura, R. D., Padalhin, A., Park, C. M., & Lee, B. (2019). Enhanced decellularization technique of porcine dermal ECM for tissue engineering applications. *Materials Science & Engineering. C, Biomimetic Materials, Sensors and Systems (Print)*, 104, 109841. <https://doi.org/10.1016/j.msec.2019.109841>
- Xu, J., Zheng, S., Hu, X., Li, L., Li, W., Parungao, R., Wang, Y., Nie, Y., Liu, T., & Song, K. (2020). Advances in the Research of Bioinks Based on Natural Collagen, Polysaccharide and Their Derivatives for Skin 3D Bioprinting. *Polymers*, 12(6), 1237. <https://doi.org/10.3390/polym12061237>